JACS
JOURNAL OF THE AMERICAN CHEMICAL SOCIETY

Subscriber access provided by ISTANBUL TEKNIK UNIV

Article

Conformation-Specific Spectroscopy and Photodissociation of Cold, Protonated Tyrosine and Phenylalanine

Jaime A. Stearns, Sbastien Mercier, Caroline Seaiby, Monia Guidi, Oleg V. Boyarkin, and Thomas R. Rizzo

J. Am. Chem. Soc., **2007**, 129 (38), 11814-11820• DOI: 10.1021/ja0736010 • Publication Date (Web): 01 September 2007

Downloaded from http://pubs.acs.org on February 14, 2009

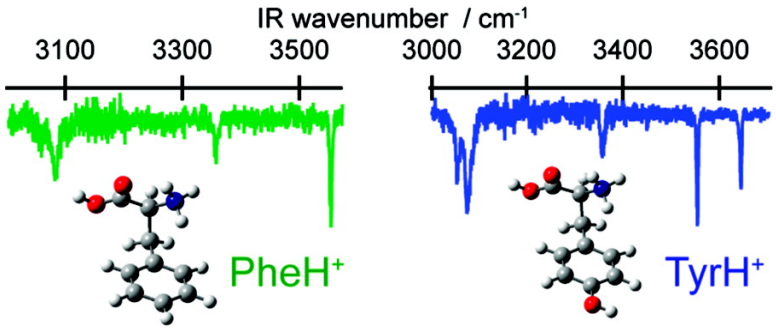

More About This Article

Additional resources and features associated with this article are available within the HTML version:

- Supporting Information
- Links to the 15 articles that cite this article, as of the time of this article download
- Access to high resolution figures
- Links to articles and content related to this article
- Copyright permission to reproduce figures and/or text from this article

View the Full Text HTML

ACS Publications
High quality. High impact.

Journal of the American Chemical Society is published by the American Chemical Society. 1155 Sixteenth Street N.W., Washington, DC 20036

J|A|C|S
ARTICLES
Published on Web 09/01/2007

Conformation-Specific Spectroscopy and Photodissociation of Cold, Protonated Tyrosine and Phenylalanine

Jaime A. Stearns,* Sébastien Mercier, Caroline Seaiby, Monia Guidi, Oleg V. Boyarkin, and Thomas R. Rizzo*

Contribution from the Laboratoire de Chimie Physique Moléculaire, Ecole Polytechnique Fédérale de Lausanne, EPFL SB ISIC LCPM, Station 6, CH-1015 Lausanne, Switzerland

Received May 19, 2007; E-mail: jaime.stearns@epfl.ch; thomas.rizzo@epfl.ch

Abstract: We present here ultraviolet and infrared spectra of protonated aromatic amino acids in a cold, 22-pole ion trap. Ultraviolet photofragmentation spectra of protonated tyrosine and phenylalanine show vibronically resolved bands corresponding to different stable conformers: two for $PheH^+$ and four in the case of $TyrH^+$. We subsequently use the resolved UV spectra to perform conformer-specific infrared depletion spectroscopy. Comparison of the measured infrared spectra to density functional theory calculations helps assign the geometry of the various conformers, all of which exhibit NH$\cdots\pi$ hydrogen bonds and NH$\cdots$O=C interactions, with the COOH group oriented either *anti* or *gauche* to the aromatic ring. In both molecules the majority of the observed fragments result from dissociation on an excited electronic state. In $TyrH^+$, different conformers excited with practically the same energy exhibit different fragmentation patterns, suggesting that the excited-state dynamics depend upon conformation.

1. Introduction

Owing to their importance in the near-UV absorption of proteins, considerable effort has been aimed at understanding the spectroscopy, structure, and excited-state dynamics of the aromatic amino acids and their derivatives. Tryptophan is the most heavily studied because of its strong absorption, high fluorescence quantum yield, and sensitivity to the local protein environment.[1−3] Although the near-UV absorption of tyrosine and phenylalanine is weaker than that of tryptophan, they occur more often in nature, and thus an understanding of their spectroscopy and photophysics is also important. The desire to understand more completely the relationships among conformation, chromophore environment, and photophysics has led to numerous gas phase spectroscopic studies of the amino acids and their derivatives in which the complicating effects of solvent have been removed.

The first electronic spectrum of a gas phase amino acid, tryptophan, was recorded in a supersonic expansion more than 20 years ago by Rizzo et al.[4] The band origins of multiple stable conformers were identified[4] and later confirmed by both ultraviolet hole-burning and infrared depletion spectroscopy.[5,6] In subsequent studies, Martinez et al. recorded electronic spectra of phenylalanine and tyrosine, identifying the band origins of 5 and 10 conformers, respectively.[7] The spectrum of tyrosine was later recorded by de Vries and co-workers at higher resolution, confirming the presence of 10 conformers,[8,9] but their spectral assignments were different than those of Martinez et al.[7] Recently, Inokuchi et al. assigned the conformers of tyrosine using infrared depletion spectroscopy, attributing the spectrum to just eight conformers.[10] In the case of phenylalanine, a combination of ultraviolet hole-burning, conformer-specific infrared spectroscopy, and rotational band contour analysis was used to assign structures to the five conformers found by Levy and identify an additional one.[11−13]

While most of these studies have probed neutral species cooled in supersonic jet expansions,[4−14] the presence of charge can have a profound effect on amino acid photophysics[15−21]

(1) Callender, R. H.; Dyer, R. B.; Gilmanshin, R.; Woodruff, W. H. *Annu. Rev. Phys. Chem.* **1998**, *49*, 173−202.
(2) Gruebele, M. *Annu. Rev. Phys. Chem.* **1999**, *50*, 485−516.
(3) Liu, T.; Callis, P. R.; Hesp, B. H.; deGroot, M.; Buma, W. J.; Broos, J. *J. Am. Chem. Soc.* **2005**, *127*, 4104−4113.
(4) Rizzo, T. R.; Park, Y. D.; Peteanu, L. A.; Levy, D. H. *J. Chem. Phys.* **1986**, *84*, 2534−2541.
(5) Snoek, L. C.; Kroemer, R. T.; Hockridge, M. R.; Simons, J. P. *PCCP* **2001**, *3*, 1819−1826.
(6) Bakker, J. M.; Aleese, L. M.; Meijer, G.; von Helden, G. *Phys. Rev. Lett.* **2003**, *91*, 3003−3003.
(7) Martinez, S. J., III.; Alfano, J. C.; Levy, D. H. *J. Mol. Spectrosc.* **1992**, *156*, 421−30.
(8) Grace, L. I.; Cohen, R.; Dunn, T. M.; Lubman, D. M.; de Vries, M. S. *J. Mol. Spectrosc.* **2002**, *215*, 204−219.
(9) Cohen, R.; Brauer, B.; Nir, E.; Grace, L.; de Vries, M. S. *J. Phys. Chem. A* **2000**, *104*, 6351−6355.
(10) Inokuchi, Y.; Kobayashi, Y.; Ito, T.; Ebata, T. *J. Phys. Chem. A* **2007**, *111*, 3209−3215.
(11) Snoek, L. C.; Robertson, E. G.; Kroemer, R. T.; Simons, J. P. *Chem. Phys. Lett.* **2000**, *321*, 49−56.
(12) Hashimoto, T.; Takasu, Y.; Yamada, Y.; Ebata, T. *Chem. Phys. Lett.* **2006**, *421*, 227−231.
(13) Lee, Y.; Jung, J.; Kim, B.; Butz, P.; Snoek, L. C.; Kroemer, R. T.; Simons, J. P. *J. Phys. Chem. A* **2004**, *108*, 69−73.
(14) Rizzo, T. R.; Park, Y. D.; Peteanu, L.; Levy, D. H. *J. Chem. Phys.* **1985**, *83*, 4819−4820.
(15) Kang, H.; Jouvet, C.; Dedonder-Lardeux, C.; Martrenchard, S.; Gregoire, G.; Desfrancois, C.; Schermann, J. P.; Barat, M.; Fayeton, J. A. *PCCP* **2005**, *7*, 394−398.
(16) Kang, H.; Dedonder-Lardeux, C.; Jouvet, C.; Martrenchard, S.; Gregoire, G.; Desfrancois, C.; Schermann, J. P.; Barat, M.; Fayeton, J. A. *PCCP* **2004**, *6*, 2628−2632.
(17) Gregoire, G.; Jouvet, C.; Dedonder, C.; Sobolewski, A. L. *Chem. Phys.* **2006**, *324*, 398−404.
(18) Boyarkin, O. V.; Mercier, S. R.; Kamariotis, A.; Rizzo, T. R. *J. Am. Chem. Soc.* **2006**, *128*, 2816−2817.

10.1021/ja0736010 CCC: $37.00 **© 2007 American Chemical Society**

and peptide conformation.[22,23] Spectroscopic studies of protonated tryptophan ($TrpH^+$) and tyrosine ($TyrH^+$) have been carried out only recently, as electrospray and ion trapping have been combined with laser techniques.[18−21] Although $TrpH^+$ is a closed shell species with an S_0-S_1 transition energy similar to that of the neutral form, the excited-state behavior of the protonated species is quite different because of an interaction between the excited $\pi\pi^*$ state and a dissociative $\pi\sigma^*$ state.[15,16] As a result of fast nonradiative decay, the electronic spectrum shows no resolved vibronic features even at low temperature.[18] The excited-state lifetime was measured to be 380 fs following 266 nm excitation, and calculations of the excited-state dynamics, as well as the broad UV spectrum of the cold species, suggest it could be even shorter.[15,18,19] The addition of two water molecules to $TrpH^+$ shifts the energy of the dissociative state and increases the excited-state lifetime, allowing the measurement of a fully vibrationally resolved electronic spectrum.[19] In contrast to protonated tryptophan, bare protonated tyrosine shows a resolved vibronic spectrum[18] and an excited-state lifetime of 22 ps subsequent to excitation at 266 nm.[15] No measurements of the spectrum of protonated phenylalanine ($PheH^+$) or its excited-state lifetime have been previously reported.

The importance of the dissociative $\pi\sigma^*$ state in the laser-induced dissociation (LID) patterns of protonated tryptophan and tyrosine has been examined in detail. The loss of a hydrogen atom is seen only in LID and can be considered a marker of dissociation on the excited $\pi\sigma^*$ surface.[15,16,20] This dissociation channel can be difficult to observe, since it leads to a fragment ion signal just one mass unit away from the much larger parent ion signal, and its presence has sometimes been inferred from secondary fragmentation to give the side chain radical cation.[16]

We report here the UV photofragment spectroscopy of $TyrH^+$ and $PheH^+$ in a 22-pole ion trap cooled to 6 K. We measure infrared spectra of both molecules using IR−UV double resonance spectroscopy and compare them with density functional theory calculations to characterize the conformations present. Our results show that the degree of excited-state fragmentation is both molecule- and conformer-dependent.

2. Experimental Approach

Figure 1 shows schematically the instrument used in these experiments. We produce gas-phase, protonated aromatic amino acids at atmospheric pressure using nanoelectrospray from a 0.2 mM solution of the amino acid in 50:50:0.2 methanol/water/acetic acid. A glass capillary with metallized ends samples the nanospray plume and conducts the ions into the vacuum chamber where they collect in a hexapole ion trap for approximately 41 ms. After being released from the hexapole, the ions pass through a quadrupole mass filter, which selects those of a particular mass-to-charge ratio (m/z). A static quadrupole deflector turns the mass-selected ions 90° and sends them through a series of deceleration lenses, and an rf-only octopole

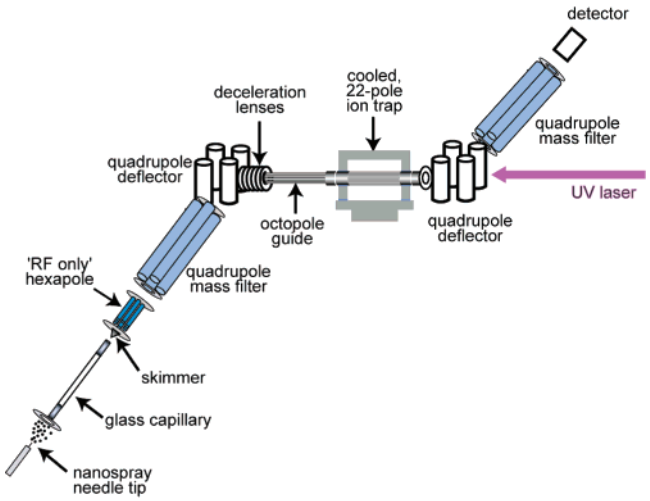

Figure 1. Schematic drawing of the photofragment mass spectrometer.

guides them into a 22-pole ion trap, which is cooled to 6 K by a closed cycle refrigerator. A pulse of helium, introduced into the trap before the arrival of the ion packet, collisionally cools the ions. After 30 ms, an ultraviolet laser pulse (or combination of IR and UV pulses) is sent through the trap to excite the cold ions. After a delay that ranges from 10 μs to 2 ms, parent ions and charged fragments resulting from absorption of a UV photon are released from the trap, turned 90°, and passed through a second quadrupole mass filter that selects either fragment ions (to monitor the photofragmentation yield) or parent ions (for normalization). The ion signal from a channeltron detector is amplified, counted, and transferred to a PC.

We record three types of data with this apparatus. In the first type, we measure electronic spectra of the parent ions by recording the photofragment ion signal as a function of the UV laser wavelength. To normalize the spectrum to the number of parent ions, we operate the UV laser at 10 Hz and the trapping cycle at 20 Hz. When the laser is on, the second quadrupole mass filter selects for a particular fragment ion, while when the laser is off it is set to pass parent ions. The latter is used to remove slow fluctuations of the nanospray ion source. For a typical laser energy of 5 mJ/pulse, the fragmentation yield is 2−5% of the parent ion signal.

In a second type of experiment, we record fragmentation mass spectra by fixing the UV laser wavelength and tuning the second quadrupole through the range of fragment masses. We record the mass spectrum with the laser on and off during alternate cycles and subtract the two.

In the third type of experiment, we record infrared−ultraviolet double resonance spectra by setting the UV laser wavelength on a particular feature in the electronic spectrum and fixing the second quadrupole to pass a particular dissociation fragment while scanning the wavenumber of an IR laser, which we also send through the trap. In this case, the UV laser runs at 20 Hz and the infrared laser runs at 10 Hz. When both lasers fire, the IR pulse precedes the UV pulse by 100 ns. When the infrared laser frequency is resonant with a ground state vibration of the conformer excited by the UV laser, IR absorption removes population from the ground state, and this is detected as a depletion in the UV-induced photofragmentation signal, which is typically 5−50% for 10 mJ IR laser pulses. We record this

(19) Mercier, S. R.; Boyarkin, O. V.; Kamariotis, A.; Guglielmi, M.; Tavernelli, I.; Cascella, M.; Rothlisberger, U.; Rizzo, T. R. *J. Am. Chem. Soc.* **2006**, *128*, 16938−16943.
(20) Talbot, F. O.; Tabarin, T.; Antoine, R.; Broyer, M.; Dugourd, P. *J. Chem. Phys.* **2005**, *122*, 074310−5.
(21) Nolting, D.; Marian, C.; Weinkauf, R. *PCCP* **2004**, *6*, 2633−2640.
(22) Jarrold, M. F. *Annu. Rev. Phys. Chem.* **2000**, *51*, 179−207.
(23) Hoaglund-Hyzer, C. S.; Counterman, A. E.; Clemmer, D. E. *Chem. Rev.* **1999**, *99*, 3037−3080.

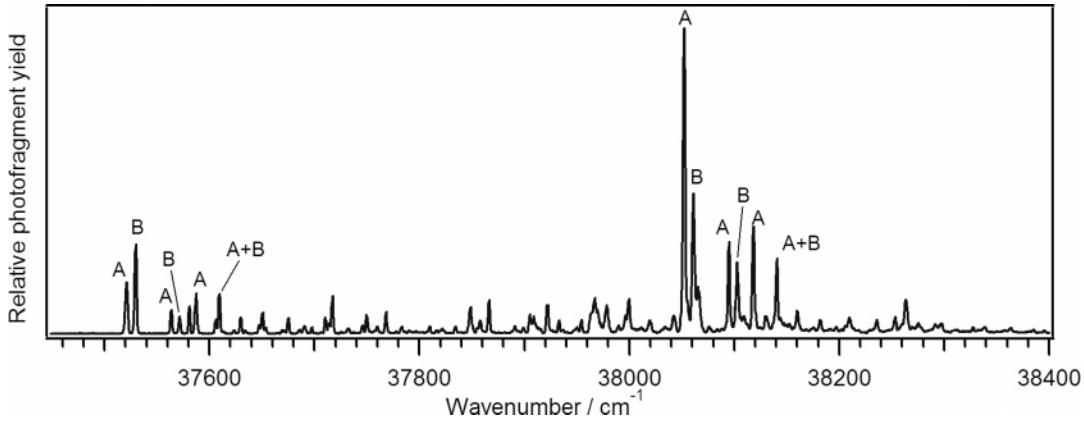

Figure 2. Ultraviolet photofragment excitation spectrum of $PheH^+$ recorded by detecting the *m*/*z* 74 fragment. The conformational assignments are based on the infrared spectra discussed in the text.

depletion as a function of IR frequency to obtain a conformer-specific infrared spectrum.

Ultraviolet light is obtained from the frequency-doubled output of a Nd:YAG-pumped Lumonics dye laser. The infrared source is a Nd:YAG-pumped LaserVision OPO/OPA.

3. Computational Methods

We performed initial conformational searches on the protonated amino acids using the AMBER force field[24] within the Macromodel program.[25] In keeping with previous calculations,[17,19,21] we assumed the protonation site to be the amino group in each case. Re-optimization of the lowest energy structures and calculation of harmonic and anharmonic vibrational frequencies were carried out using B3LYP/6-31++G** in Gaussian03.[26] Harmonic hydride stretch frequencies were scaled by 0.954 for comparison to the infrared spectra, but all frequencies were left unscaled in the zero-point energy calculations. Anharmonic frequency calculations were left unscaled.

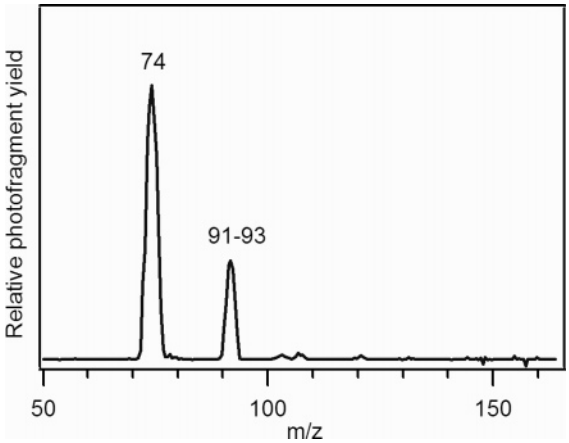

Figure 3. Photofragment mass spectrum of $PheH^+$. The *m*/*z* of the major fragments are labeled. Note that the parent mass is 166 amu.

4. Experimental Results

4.1. Phenylalanine. Figure 2 shows the vibrationally resolved ultraviolet photofragmentation spectrum of $PheH^+$ monitoring the fragment at *m*/*z* 74. The first origin transition at 37 520.9 cm^{-1} occurs only 17 cm^{-1} to the red of that of the neutral species. The second peak in the UV spectrum of $PheH^+$ (37 529.6 cm^{-1}) is larger than the first but does not appear as part of a Franck−Condon progression. Together with the small energy difference between the first two peaks, this suggests that it is the origin transition of a different conformer.

Excitation of the first two UV transitions of $PheH^+$ (37 520.9 cm^{-1} and 37 529.6 cm^{-1}) results in the same fragmentation mass spectrum, shown in Figure 3. The most intense fragment signal is centered at *m*/*z* 74, which corresponds to $NH_2-CH-COOH$, the radical cation left upon loss of a hydrogen atom and breakage of the $C_\alpha-C_\beta$ bond. This fragment is much less prominent in photofragmentation of the other protonated aromatic amino acids and is not observed in collision-induced dissociation (CID).[27] The other major fragment is spread over the mass channels 91−93. Mass 93 is observed in CID and is attributed to the loss of (H_2O + CO + HCN).[27] Mass 91 corresponds to the side chain radical cation,[15] but it is not clearly distinguishable from *m*/*z* 93, since we run our analyzing quadrupole at relatively low resolution to maximize ion transmission. The UV spectrum is identical when recorded at *m*/*z* 91−93 or *m*/*z* 74. At the mass resolution of these experiments, we cannot detect the fragmentation channel corresponding to the loss of hydrogen.[15]

Figure 4 shows the infrared spectrum associated with the first UV transition of $PheH^+$ (37 520.9 cm^{-1}). Several calculated spectra are displayed below the experimental spectrum, each representing a family of structures classified according to the NH_3 and COOH orientations. The global minimum (Figure 4a) contains two stabilizing hydrogen-bond interactions of the charged NH_3 group, one with the π-cloud of the ring and one with the carbonyl oxygen. Rotation of the carboxylic acid group results in an NH···OH interaction (Figure 4b) that is considerably weaker than the NH···O=C interaction (Figure 4a), increasing the energy of the ion by 16.0 kJ/mol and shifting the NH stretching frequency up from 3188 cm^{-1} to 3283 cm^{-1}. The loss of the NH···π interaction in the conformers shown in Figure 4c and d also results in a higher frequency NH stretch and considerably higher energies. Only the lowest energy structure (Figure 4a) is consistent with the experimental spectrum. There are two structures with NH_3 and COOH orientations like that of Figure 4a that differ in the orientation of the backbone with respect to the ring by a rotation of the angle χ_1. The structure with $\chi_1 = 72°$ (*gauche*) is 3.2 kJ/mol

(24) Cornell, W. D.; Cieplak, P.; Bayly, C. I.; Gould, I. R.; Jr., K. W. M.; Ferguson, D. M.; Spellmeyer, D. C.; Fox, T.; Caldwell, J. W.; Kollman, P. A. *J. Am. Chem. Soc.* **1995**, *117*, 5179−5197.
(25) *MacroModel*, version 9.1; Schrödinger, LLC: New York, 2005.
(26) Frisch, M. J., et al. *Gaussian 03*, revision B.03; Gaussian, Inc.: Pittsburgh, PA, 2003.
(27) El Aribi, H.; Orlova, G.; Hopkinson, A. C.; Siu, K. W. M. *J. Phys. Chem. A* **2004**, *108*, 3844−3853.

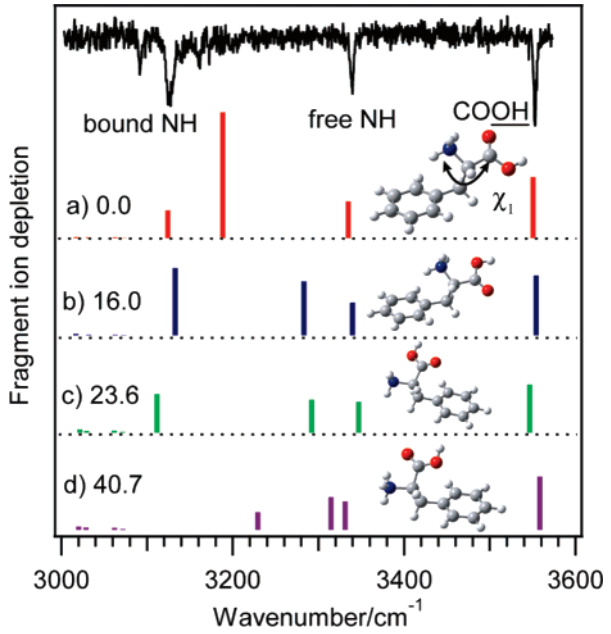

Figure 4. Infrared spectra of $PheH^+$ in the hydride stretch region. Top: experimental spectrum of conformer A. Spectra calculated at the B3LYP/6-31++G** level of theory are shown in (a)−(d) for four families of conformers, with the zero-point corrected energy of each structure in kJ/mol. The dihedral angle χ_1 is shown in part (a).

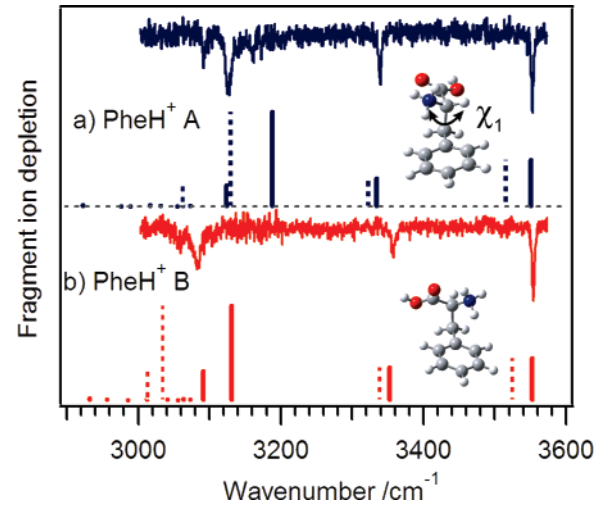

Figure 5. Infrared spectra of conformers (a) A and (b) B of $PheH^+$. Calculated spectra (B3LYP/6-31++G**) and structures are shown below the experimental spectra. The solid line spectra represent scaled harmonic frequencies, and the dashed line spectra are unscaled anharmonic frequencies. The dihedral angle χ_1 is shown in part (a).

higher in energy than the global minimum structure, which has $\chi_1 = 169°$ (*anti*).

Figure 5 displays the infrared spectra associated with the first two transitions in the UV spectrum. While the peak corresponding to the carboxylic acid OH stretch is indistinguishable between the two, the vibrational frequency of the noninteracting ammonium NH stretch differs by 15 cm^{-1}, supporting the assertion that the peaks in the UV spectrum belong to different conformers. Further differences occur in the lower frequency region, where the vibrational bands of the NH groups interacting with the π cloud and the carboxyl group appear. Comparison with the anharmonic and scaled harmonic calculated frequencies for $PheH^+$ suggests assigning the spectrum of Figure 5a to conformer A, which corresponds to the global minimum *anti* structure, and that of Figure 5b to conformer B, the *gauche* structure. We make this assignment based upon the good agreement between the calculated and observed free NH stretch frequencies as well as the prediction that the hydrogen-bonded NH stretches are further shifted to the red in conformer B. This assignment is further supported by the correct prediction of the greater splitting between the bound NH stretches in conformer A compared to those of conformer B. We obtained similar infrared spectra to help assign the conformers associated with many of the transitions in the UV spectrum of Figure 2.

The electronic spectra of both conformers exhibit a hot band (at −43.6 cm^{-1} for A and −42.9 cm^{-1} for B), which is too small to be observed on the scale of Figure 2. Using the intensity of this hot band, we estimate a vibrational temperature of $PheH^+$ of ∼12 K, which is similar to that determined for protonated tyrosine.[18] A vibrational mode of similar frequency in the excited state (43.6 cm^{-1} for A and 42.0 cm^{-1} for B) seems to be built off of the origin for each conformer. The lowest frequency vibration predicted by our calculations is a torsion of the phenyl ring with respect to the backbone that has a ground state harmonic frequency of 45 cm^{-1} for conformer A and 43 cm^{-1} for conformer B. Conformer A shows considerably more vibronic activity than conformer B, indicating a larger geometry change upon excitation. The low-frequency vibrations are also built off of the large vibronic bands at 38 052.4 cm^{-1} and 38 061.1 cm^{-1}, which are 531 cm^{-1} above the band origins of conformers A and B, respectively. This vibrational mode corresponds well to the *6b* vibration of benzene and its derivatives, which appears at 530 cm^{-1} in the excited state of toluene.[28] The intensity of this transition in toluene and other substituted benzenes derives from vibronic coupling between the L_b and L_a $\pi\pi^*$ excited states, and this is likely also the case for $PheH^+$. The relative sizes of the origins and *6b* bands for conformers A and B of $PheH^+$ may indicate that the coupling is stronger for conformer A, giving rise to a larger *6b* band despite a smaller origin.

4.2. Tyrosine. Figure 6 shows two UV photofragmentation spectra of $TyrH^+$. Figure 6b was recorded by monitoring the fragment at *m*/*z* 136, which corresponds to the loss of CO + H_2O, the major channel in CID.[27] This channel also has been observed in laser-induced dissociation.[15] Figure 6a was recorded by monitoring the fragmentation into *m*/*z* 107, which corresponds to the tyrosine side chain radical cation, a fragment previously identified as a marker of excited-state fragmentation[15] and which only appears as a minor product in CID. The same UV transitions occur in both spectra of $TyrH^+$, but the relative intensities of the transitions depend on the detected fragment. This complementarity of the peak intensities between these two spectra, together with the lack of any systematic energy threshold for the opening of new fragmentation channels, strongly suggests that multiple conformers are responsible for the features in the electronic spectrum and that some of these conformers must exhibit different fragmentation patterns.

The fragmentation mass spectra recorded with the UV wavelength fixed to the first two transitions (35 081.3 cm^{-1}, Figure 7a, and 35111.4 cm^{-1}, Figure 7b) confirm that they are associated with conformers exhibiting different fragmentation behavior. Despite a difference in UV excitation energy of only

(28) Hopkins, J. B.; Powers, D. E.; Smalley, R. E. *J. Chem. Phys.* **1980**, *72*, 5039−5048.

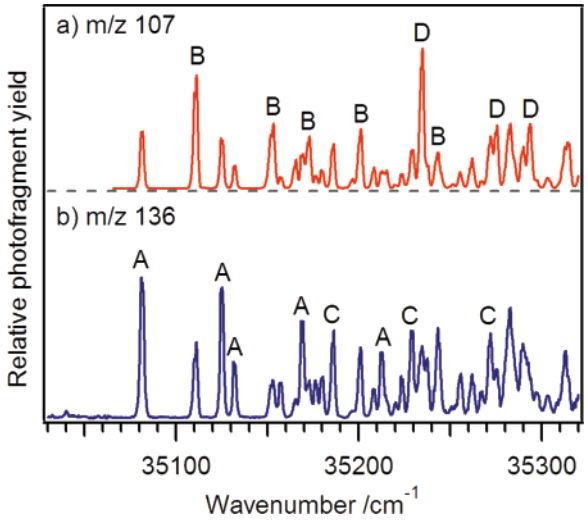

Figure 6. Ultraviolet photofragment excitation spectra of $TyrH^+$ recorded using the fragment at (a) *m*/*z* 107 and (b) *m*/*z* 136. The conformational assignments discussed in the text are labeled A−D. The same transitions appear in both spectra, but the labels are not reproduced in both for the sake of clarity.

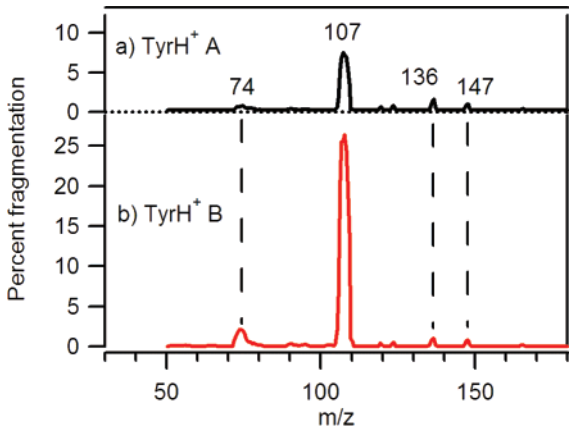

Figure 7. Fragment mass spectra of $TyrH^+$ recorded at (a) 35 081.5 cm^{-1} and (b) 35 111.4 cm^{-1}. The *m*/*z* of the major fragments are labeled. The mass of the parent $TyrH^+$ is 182 amu.

30 cm^{-1}, the *m*/*z* 107 fragment is almost four times larger when produced by excitation of the second UV transition than by excitation of the first. We assign these transitions to different conformers of $TyrH^+$, designated A and B, and further confirm this assignment by IR−UV double-resonance spectroscopy.

Figure 8a and b show the infrared spectra associated with the first two transitions in the UV spectrum of $TyrH^+$. These spectra differ in the free and bound NH stretch regions, which signals a difference in the backbone orientation. Based on the agreement with the calculated frequencies, we assign conformer B to the global minimum *anti* structure with $\chi_1 = 178°$ and conformer A to the *gauche* structure with $\chi_1 = 73°$, 2.7 kJ/mol higher in energy. These are similar to the low-energy conformers of $PheH^+$, both in their backbone orientation and the presence of NH···π and NH···O═C hydrogen bonds.

Compared to $PheH^+$, the two possible orientations of the phenolic OH group in $TyrH^+$ should double the number of low-energy conformers. Indeed, our calculations predict the existence of third and fourth conformers that differ from A and B in this way. A careful analysis of the UV spectrum and the subtle differences in the bound NH stretch region of the IR spectra allow us to locate the electronic band origins of two additional conformers, C and D, at 35 186.4 cm^{-1} and 35 234.9 cm^{-1}, repectively. The UV transition at 35 234.9 cm^{-1} is the largest band in the spectrum but does not appear as part of any vibrational progression. The infrared spectrum associated with this transition (Figure 8d) is clearly similar to conformer B, but the largest peak in the bound NH stretch region appears at 3129 cm^{-1} in conformer B and 3127 cm^{-1} in conformer D. We thus assign the structure of conformer D to one similar to conformer B, with an *anti* orientation of χ_1, but with the opposite OH orientation. The calculations predict the structure with the hydroxyl lone pair *syn* to the NH_3 group to have a bound NH stretch only 0.5 cm^{-1} higher in frequency than that with the lone pair *anti* to the NH_3 group. We thus cannot determine the absolute orientation of the OH.

The IR spectrum associated with the transition at 35 186.4 cm^{-1} proves that it belongs to a fourth conformer (C). The differences between conformers A and C in the bound NH stretch region are more substantial than those between B and D. The most intense bound NH stretch in A has a frequency of 3086 cm^{-1} while that of C is 3076 cm^{-1}. Calculations indicate the conformer with the phenolic oxygen lone pair in the *syn* configuration has a bound NH stretch frequency 3 cm^{-1} higher than the bound NH stretch frequency of the *anti* conformer. This difference is too small to allow us to assign the OH orientation.

Obtaining an IR−UV double resonance spectrum for each peak in the UV spectrum allows us to associate them with one of these four conformations, as labeled in Figure 6. All four conformers exhibit a low-frequency progression around 42 cm^{-1} with more extensive vibronic activity than that in $PheH^+$. There is also a low-frequency vibration around 52 cm^{-1} in each conformer, although for conformer C this vibronic peak is likely hidden by the origin of conformer D. These peaks correspond well to the lowest frequency calculated ground state vibrations, which are both torsions of the ring and backbone.

5. Discussion

5.1. Conformations. The protonated aromatic amino acids are closed shell species with ultraviolet chromophores and $\pi\pi^*$ excitation energies similar to those of the neutrals. Protonation results in a red shift of the S_0-S_1 transition energies of about 400 cm^{-1} for the various tyrosine conformers and about 50 cm^{-1} for phenylalanine, indicating the $\pi\pi^*$ state does not depend strongly on the protonation state for these species.

Only the lowest energy calculated structures were found in the experiment, suggesting the cooling process does not trap molecules in higher energy potential minima. The conformations observed for $TyrH^+$ and $PheH^+$ belong to the same families, each having two backbone orientations, with dihedral angle $\chi_1 = \sim 170°$ (*anti*) and $\sim 70°$ (*gauche*). The two conformers of $PheH^+$ found in the present experiment are analogous to conformers II and VII calculated for the neutral species, although VII was not observed in a gas-phase experiment.[11] The conformers of $TyrH^+$ are the same as neutral conformers D and E observed by Inokuchi et al.[10] Fewer stable conformers occur for the protonated species than in the neutrals because of the strong interactions involving the charged ammonium group. Conformations of the protonated aromatic amino acids that contain hydrogen bonding between the ammonium group and

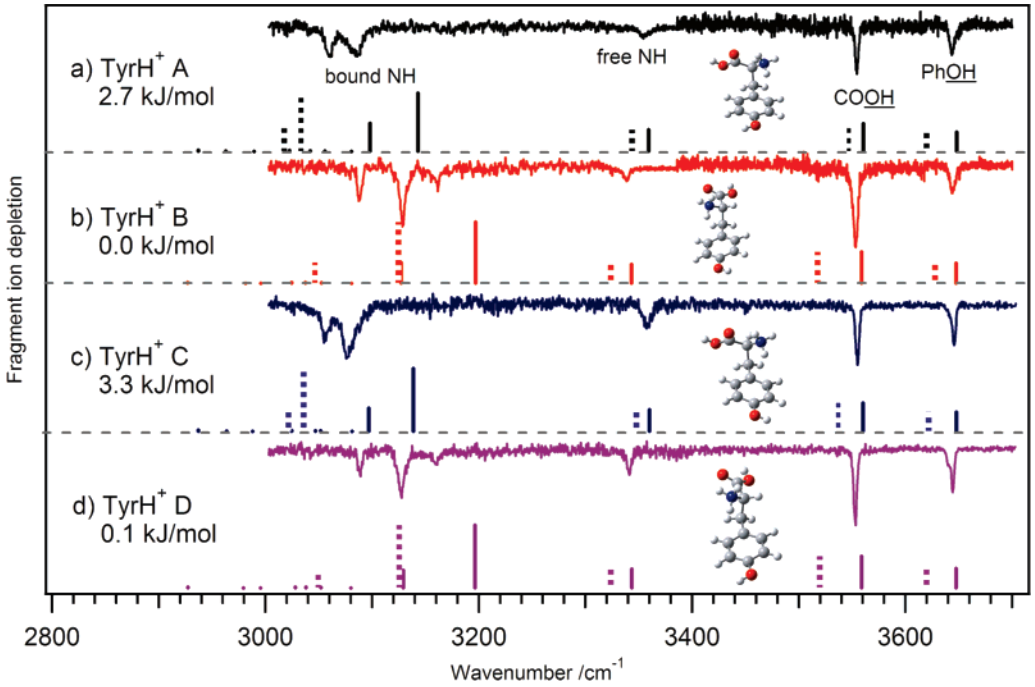

Figure 8. Infrared spectra of $TyrH^+$. Calculated (B3LYP/6-31++G**) spectra and structures are shown below the experimental spectrum for each conformer. The more intense of the bound NH stretches of conformers A and C differ by 12 cm^{-1}, while those of B and D differ by 2 cm^{-1}. Scaled harmonic frequencies are shown as solid line spectra, and unscaled anharmonic frequencies are shown as dashed line spectra.

the π cloud of the aromatic ring or the carbonyl oxygen are stabilized by 15−40 kJ/mol. In addition, many of the observed, low-energy conformers of the neutral species have a hydrogen bond between the carboxylic acid OH and the lone pair on the amino group, which does not exist in the protonated molecules.

Though the orientation of the phenolic OH in $TyrH^+$ has only a small effect on the ground state energy (as suggested by our calculations), it has a more significant effect on the excited state. Conformers A and C, which differ only by the OH orientation, have electronic origin transitions split by 105 cm^{-1}, and those of B and D are split by 123 cm^{-1}. This splitting is similar to that in the neutral molecules 5-hydroxyindole[29] and serotonin[30] but larger than the splitting measured for neutral tyrosine.[10] In both $TyrH^+$ and $PheH^+$, the rotation of the backbone angle χ_1 has a small effect on the excitation energy, less than 50 cm^{-1} in all cases.

The infrared spectra shown in Figures 5 and 8 match well with the calculated spectra in the OH and free NH stretching regions when the harmonic frequencies are scaled by a universal factor of 0.954. However, this approach consistently overestimates the frequencies of the red-shifted NH stretch bands. One reason may be that DFT underestimates the NH···π interaction, and one might think that MP2 would be better. We have found, however, that MP2 gives higher-frequency bound NH stretches for both $TyrH^+$ and $PheH^+$, resulting in a worse agreement with experiment. It seems more likely that the anharmonicity of the N−H bond increases as a result of the interaction between the charged ammonium group and the π cloud, decreasing the stretching frequency. We thus performed anharmonic frequency calculations, the results of which are shown in Figures 5 and 8. The unscaled anharmonic frequencies differ from our measured values by no more than 2%. The agreement with experiment in the hydrogen-bonded NH stretch region is considerably better than the scaled harmonic frequencies for conformer A of $PheH^+$ and conformers B and D of $TyrH^+$, all of which have the same backbone orientation.

5.2. Excited-State vs Ground-State Fragmentation. The most abundant fragments observed in both $TyrH^+$ and $PheH^+$ involve cleavage of the $C_\alpha-C_\beta$ bond, giving predominately the side chain radical cation (*m*/*z* 107) in the case of $TyrH^+$ and the amino acid backbone radical cation ($NH_2-CH-COOH$, *m*/*z* 74) in the case of $PheH^+$. Because neither of these fragments is abundant in the CID fragment distributions reported by El Aribi et al.,[27] which were recorded under single-collision conditions at center-of-mass energies up to 8 eV, they must result from dissociation on an excited electronic state. The mechanisms of excited-state fragmentation have been studied in detail for $TrpH^+$ and $TyrH^+$, with a dissociative $\pi\sigma^*$ state playing a key role.[15,16,31] The bright $\pi\pi^*$ state is coupled to the $\pi\sigma^*$ state, which corresponds to electron transfer from the aromatic ring to the ammonium group. Several processes are possible following electron transfer, including proton transfer to the aromatic ring leading to internal conversion, loss of neutral hydrogen atom, or proton or H-atom transfer to the carbonyl oxygen. In $TyrH^+$ all but the proton transfer to the ring have been calculated to involve significant barriers,[31] suggesting internal conversion should dominate. The mechanism of the excited-state dissociation that we observe is thus unclear.

Calculations on the two conformer families of $TyrH^+$ predict different $\pi\sigma^*$ state energies,[31] although the conformer with the lower $\pi\sigma^*$ state (*gauche*) is the one for which we observe less excited-state fragmentation. Thus, the conformer-specific fragmentation that we observe may not be the result of different $\pi\pi^*-\pi\sigma^*$ coupling but rather different barriers to the proton

(29) Arnold, S.; Sulkes, M. *Chem. Phys. Lett.* **1992**, *200*, 125−129.
(30) LeGreve, T. A.; Baquero, E. E.; Zwier, T. S. *J. Am. Chem. Soc.* **2007**, *129*, 4028−4038.
(31) Gregoire, G.; Jouvet, C.; Dedonder, C.; Sobolewski, A. L. *J. Am. Chem. Soc.* **2007**, *129*, 6223−6231.

or H-atom transfer which change the branching ratio between excited-state fragmentation (*m*/*z* 107) and ground-state fragmentation (*m*/*z* 136). The lack of conformer-specific fragmentation in $PheH^+$ may simply reflect the fact that all of the observed fragmentation occurs in the excited state. One consequence of the prominent excited-state dissociation is that larger peptide ions containing these chromophores may also have similar fragmentation pathways, in which case the dissociation rate would not scale with the size of the molecule. This would allow us to extend our photofragmentation techniques to larger molecules that otherwise might not dissociate on the tens-of-milliseconds time scale of our experiment.

6. Conclusions

We have recorded ultraviolet spectra and conformation-specific infrared spectra of the protonated aromatic amino acids phenylalanine and tyrosine in a cold 22-pole ion trap. On the basis of the infrared spectra and DFT calculations, we determined there are two conformations of $PheH^+$ and four conformations of $TyrH^+$ present in our experiment, all of which are stabilized by hydrogen bonding between the charged NH_3 group and the aromatic ring and carbonyl oxygen. The peptide backbone is found in two conformations relative to the aromatic ring in each amino acid. These two orientations give rise to different fragmentation patterns in $TyrH^+$, indicating conformation-specific excited-state fragmentation.

Acknowledgment. Funding was generously provided by the École Polytechnique Fédérale de Lausanne and the Fonds National Suisse through Grant No. 200020-112071.

Supporting Information Available: Complete ref 26. This material is available free of charge via the Internet at http://pubs.acs.org.

JA0736010